Single-particle excitations in the level structure of ^{64}Cu

S. Samanta, S. Das, R. Bhattacharjee, S. Chatterjee, R. Raut,[*] and S. S. Ghugre
UGC-DAE Consortium for Scientific Research, Kolkata Centre, Kolkata 700098, India

A. K. Sinha
UGC-DAE Consortium for Scientific Research, University Campus, Khandwa Road, Indore 452017, India

U. Garg
Department of Physics, University of Notre Dame, Notre Dame, Indiana 46556, USA

Neelam
Department of Physics and Astrophysics, University of Delhi, New Delhi 110007, India

N. Kumar
Amity Institute of Nuclear Science and Technology, Amity University, Noida 201303, India

P. Jones
Department of Subatomic Physics, iThemba Labs, Somerset West 7129, South Africa

Md. Sazedur R. Laskar, F. S. Babra, S. Biswas, S. Saha, P. Singh, and R. Palit
Tata Institute of Fundamental Research, Mumbai 400005, India

Excited states of the ^{64}Cu ($Z = 29, N = 35$) nucleus have been probed using heavy-ion-induced fusion evaporation reaction and an array of Compton-suppressed Clovers as detection system for the emitted γ rays. More than 50 new transitions have been identified and the level scheme of the nucleus has been established up to an excitation energy $E_x \sim 6$ MeV and spin $\sim 10\hbar$. The experimental results have been compared with those from large-basis shell-model calculations that facilitated an understanding of the single-particle configurations underlying the level structure of the nucleus.

I. INTRODUCTION

Nuclear structure pursuits in the vicinity of the doubly magic ^{56}Ni ($Z = 28, N = 28$) core have been of much interest and have yielded exciting results. With few nucleons outside the Ni core, the low-spin domain of these nuclei exhibit complex irregular excitation patterns, typical of shell-model configurations, based on $p_{3/2}$, $f_{5/2}$, $p_{1/2}$, and $g_{9/2}$ orbitals. At higher excitations, availability of high-spin orbitals may lead to observation of deformed rotational bands, based on multiquasiparticle excitations across the $N = Z = 28$ closure, and their termination from the complete alignment of the individual particle angular momenta [1,2]. There is precedence of observation of a rich panorama of single-particle and collective modes of excitations, including exotic phenomenon such as magnetic rotation (MR), coexisting in the same nucleus, such as ^{60}Ni ($Z = 28, N = 32$) [3], in this region. Such prospects do provide an impetus for spectroscopic endeavors aimed at level structure investigations of these nuclei around the Ni core.

The present paper reports results from γ-ray spectroscopic studies of the ^{64}Cu ($Z = 29, N = 35$) nucleus, following its population in a heavy-ion-induced fusion-evaporation reaction and using a large array of Compton-suppressed Clover γ-ray detectors. This is the first instance wherein the nucleus has been studied through a heavy-ion reaction with such high resolution at an efficient detection facility. The last spectroscopic studies of the nucleus date back to 1970s and were carried out using light-ion reactions along with modest detection setups, typically based on a small number of NaI(Tl) and/or Ge(Li) detectors. These early efforts by Chan *et al.* [4], Green *et al.* [5], and Bleck *et al.* [6] could identify a limited excitation scheme of the nucleus up to a level energy of $E_x \sim 4$ MeV, with no or tentative spin-parity assignments for most of the states. A probe into the excitations of ^{64}Cu and the angular momentum generation mechanism therein, using the contemporary spectroscopy tools, is thus warranted. The results may provide a comparison with the existing nuclear structure systematics of the region and facilitate validation of nuclear models, such as the shell model, invoked for interpretation of the experimental observations.
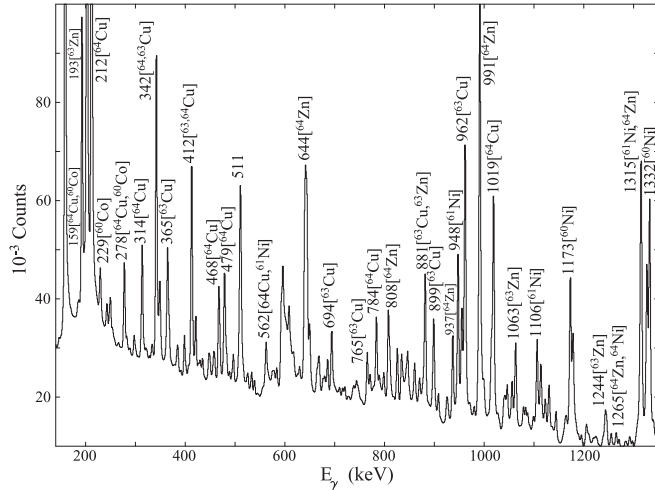
[*]rraut@alpha.iuc.res.in

FIG. 1. Part of the projection spectrum constructed out of the present data illustrating the different nuclei populated in the experiment.

FIG. 2. R_{ADO} values for different transitions of ^{64}Cu along with those of selected transitions of previously known multipolarities from other nuclei populated in the present experiment. The latter is used to fix the reference values used in the current analysis as well as for validation of the same.

II. EXPERIMENTAL DETAILS AND DATA ANALYSIS

The ^{64}Cu nucleus was populated using the ^{59}Co(^{7}Li, pn)^{64}Cu reaction at E_{lab} = 22–24 MeV. The ^{7}Li beam was obtained from the Pelletron LINAC Facility at the Tata Institute of Fundamental Research (TIFR), Mumbai. The target, fabricated at the TIFR Target Laboratory, was 5.2 mg/cm^2 of monoisotopic ^{59}Co evaporated on a 4 mg/cm^2 thick Ta foil. The γ rays from the de-exciting nuclei were detected using an array of 11 Compton-suppressed Clover detectors positioned at 90° (4 detectors), 115° (1 detector), 140° (3 detectors), and 157° (3 detectors). The pulse processing and data acquisition system was one based on Pixie-16 100-MHz 12-bit digitizers from XIA LLC, USA [7]. In-beam list-mode data were acquired under the trigger condition of at least two Clovers firing in coincidence and $\sim$1 × 10^9 events of multiplicity $\geqslant$2 were recorded during the experiment.

Figure 1 illustrates a part of the raw projection spectrum constructed from the acquired data indicating the wide range of different nuclei populated in the reaction used in the present work. The relative population of ^{64}Cu, through pn evaporation channel, was $\sim$70% of the most dominant $2n$ evaporation channel leading to the production of ^{64}Zn. The acquired data were sorted into symmetric and angle-dependent γ-γ matrices as well as γ-γ-γ cube for extraction of coincidence information between the observed γ rays and for determination of their angular correlation and linear polarization, for identifying their multipolarity and electromagnetic character. This information is used to deduce the level structure of the nuclei of interest. The sorting procedure was carried out using the MARCOS code [7] while the RADWARE [8] package was used for data analysis.

The multipolarities of the γ-ray transitions were assigned from their ratio of angular distribution from oriented nuclei (R_{ADO}) [9], defined as

$$R_{ADO} = \frac{I_{\gamma 1} \text{ at } 140° \text{ (Gated by } \gamma_2 \text{ at all angles)}}{I_{\gamma 1} \text{ at } 115° \text{ (Gated by } \gamma_2 \text{ at all angles)}}, \quad (1)$$
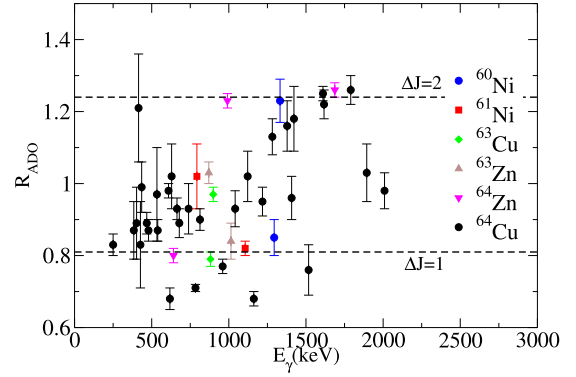
where $I_{\gamma 1}$ indicates the intensity of the γ-ray transition of interest. Two asymmetric, angle-dependent matrices were constructed for determination of the R_{ADO} values. These had γ rays detected by all detectors on the x axis and those detected in coincidence at 140° (115°) detectors on the y axis. In the present setup, the expected value of R_{ADO} for pure quadrupole transitions is 1.24 ± 0.02 and that for pure dipole transitions is 0.81 ± 0.01. These were determined from the weighted average of the quantity calculated for γ-ray transitions of previously known pure multipolarities and belonging to other dominant reaction products, such as ^{64}Zn and ^{60,61}Ni, populated in the present experiment. A R_{ADO} value between those for pure transitions, 0.81 and 1.24, would indicate mixed multipole nature with mixing ratio, $\delta > 0$, while a value less than 0.81 would signify a negative mixing ratio. Figure 2 illustrates the plot of R_{ADO} values of γ-ray transitions from ^{64}Cu along with those used to determine the reference values. The multipolarity assignments based on these numbers are discussed in the subsequent section.

The use of Clover detectors facilitated extraction of linear polarization information on the observed γ rays, albeit with higher uncertainties owing to the limited number of detectors at 90° that are used for the purpose. The polarization of a γ-ray transition is indicative of its electromagnetic (electric or magnetic) character and is determined from the asymmetry (Δ) between its scattering in the perpendicular and the parallel planes with respect to the reaction plane. The asymmetry is quantitatively defined as

$$\Delta = \frac{aN_\perp - N_\parallel}{aN_\perp + N_\parallel}, \quad (2)$$

where $N_\perp$ and $N_\parallel$ are the number of scattered photons, of a given γ ray, perpendicular and parallel to the reference plane, respectively. The term a is the geometrical asymmetry (inherent) in the detection setup and is expressed as
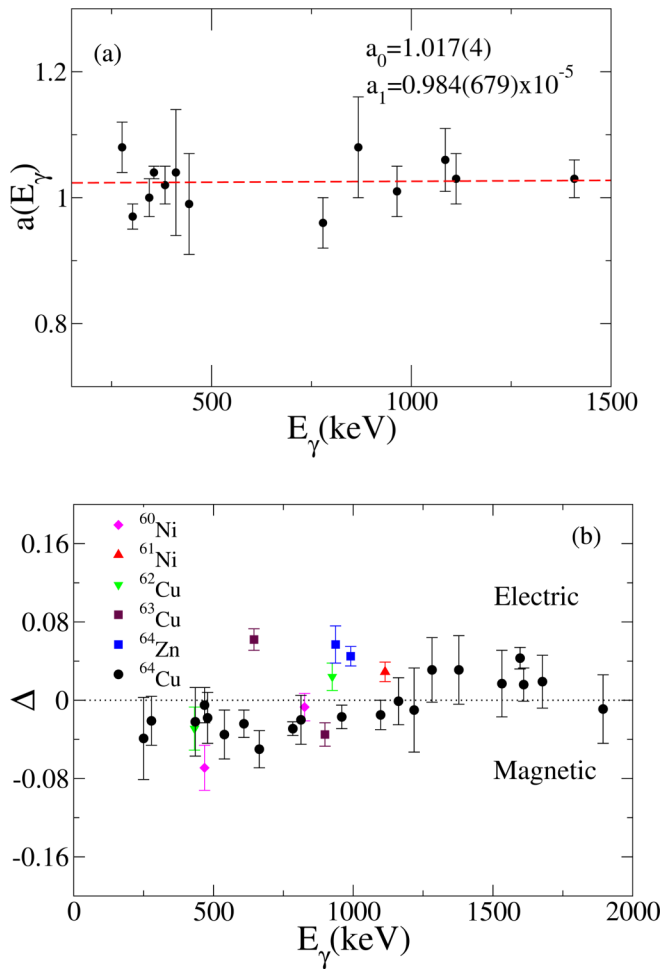
$$a = \frac{N_\parallel}{N_\perp} \quad (3)$$

FIG. 3. (Upper panel) Plot of the geometrical asymmetry (*a*) against γ-ray energies along with the fit to the data points using the equation $a_0 + a_1 E_\gamma$. (Lower panel) Plot of polarization asymmetry Δ [defined in Eq. (2)] for different γ-ray transition in ^{64}Cu along with those in other dominantly produced nuclei in the same experiment, included as reference.

FIG. 4. (Upper panel) Plot of polarization sensitivity as a function of γ-ray energy, determined from the observed γ rays of previously known multipole mixing ratio, along with the fit using Eq. (5). (Lower panel) Plot of polarization P, defined in Eq. (4), for different γ-ray transitions of ^{64}Cu and other nuclei populated in the present experiment. The latter are of previously known multipole mixing that were used to calculate their theoretical polarization, included in the plot, for reference and validation of the current analysis.

with respect to the scattering of γ rays from an unpolarized radioactive source. This was determined to be 1.017 ± 0.004 from fitting the data points [Fig. 3(a)], obtained using ^{152}Eu and ^{133}Ba sources, with the equation $a_0 + a_1 E_\gamma$; $a_1 = 0.984 \pm 0.679 \times 10^{-5}$ was insignificantly small and was ignored in the calculation of Δ. Two asymmetric matrices were constructed for extraction of the polarization asymmetry (Δ). These had γ rays detected by all detectors on the *x* axis and those detected in coincidence by the perpendicular (parallel) combination of crystals in the 90° detectors on the y-axis. Figure 3(b) depicts the Δ values for the γ-ray transitions of ^{64}Cu along with those of previously known electromagnetic nature which are included as validation of the current analysis. A positive value of Δ is indicative of an electric nature while a negative value implies that the γ-ray transition is magnetic. A near-zero Δ usually signifies a mixed electromagnetic character. However, it may be noted that the value of Δ extracted from the difference in the (Compton) scattering in perpendicular and parallel directions would be dependent on the energy of the incident γ
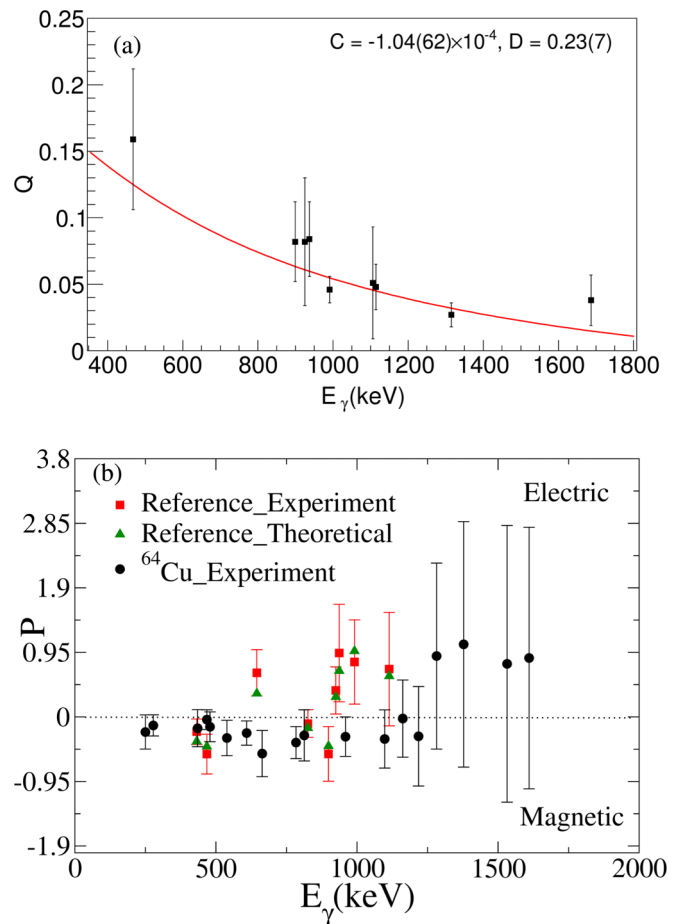
ray. This dependence can be done away with by normalizing the asymmetry with what is called the polarization sensitivity (Q) and defining the polarization (P) as

$$P = \frac{\Delta}{Q}, \tag{4}$$

where

$$Q(E_\gamma) = Q_0(E_\gamma)(C E_\gamma + D) \tag{5}$$

with

$$Q_0(E_\gamma) = \frac{\alpha + 1}{\alpha^2 + \alpha + 1} \tag{6}$$

and $\alpha = E_\gamma / m_e c^2$, with $m_e c^2$ being the electron rest mass energy. The C and D parameters, required to determine the polarization sensitivity for a given incident γ-ray energy, were extracted from a fit of the sensitivity data for transitions of
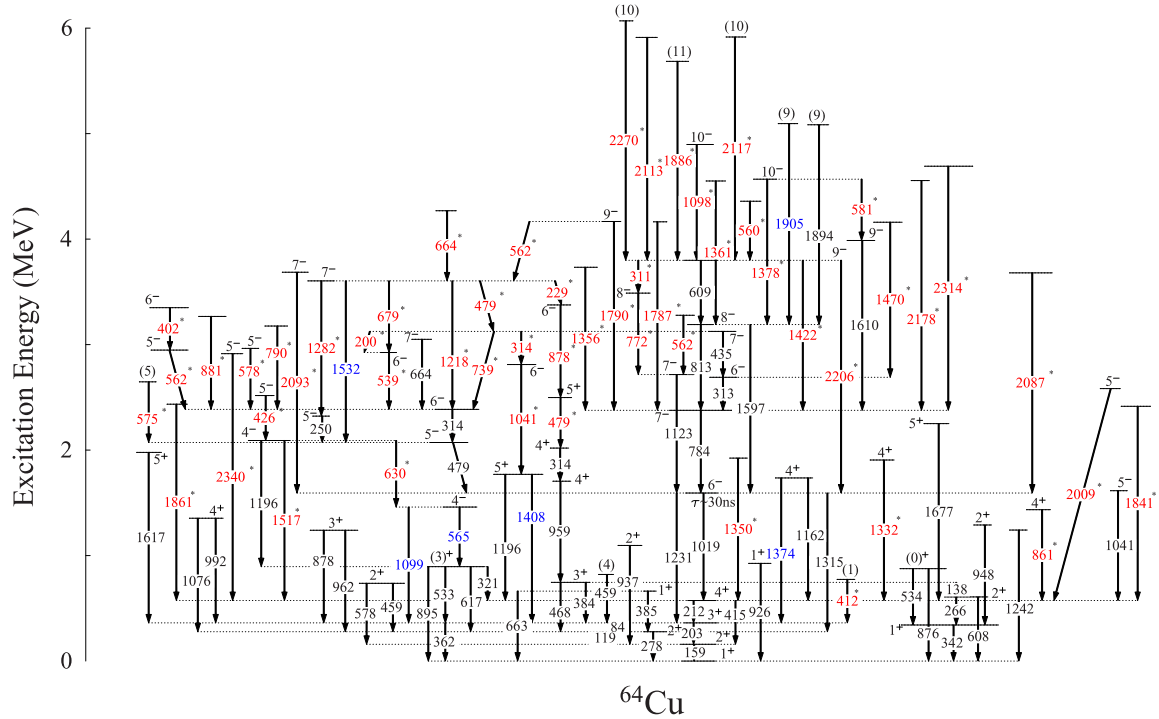
FIG. 5. Level scheme of the ^{64}Cu nucleus from the present work. The new γ-ray transitions identified from the current study are marked with * and labeled in red. The transitions labeled in blue were observed in the previous studies but were either not placed in the level scheme or had different placement with respect to the energy and/or J^π values of the de-exciting states.

previously known multipolarity, electromagnetic character, and mixing ratio, observed in the present measurements. The sensitivity for these γ-ray transitions were calculated using Eq. (4) following the determination of their Δ, using Eq. (2), and (theoretical) P using the prescription of Ref. [10]. Figure 4(a) illustrates the plot of the sensitivity Q against γ-ray energy, from the present data, along with the fit using Eq. (5). The corresponding fitted parameters are $C = (-1.04 \pm 0.62) \times 10^{-4}$ and $D = 0.23 \pm 0.07$. These were used to determine the polarization P of the transitions of ^{64}Cu and of some of the other nuclei, populated in the experiment, and the same are plotted in Fig. 4(b). Identical to that inferred from the sign of the Δ value, a positive P indicates electric transition, a negative one implies magnetic nature, and a near-zero value is interpreted as representing a mixed character. The plot also includes theoretical polarization values for the transitions that are of previously known multipole mixing ratio and belonging to other nuclei dominantly populated in the present experiment, calculated using the expressions of Ref. [10]. The overlap between the theoretical and experimental P values for these cases is found to be satisfactory and provides further validation to the polarization values extracted in the current analysis.

Following the coincidence relationships between the observed γ-ray transitions, their intensities, their multipolarities from the R_{ADO} measurements, and their electromagnetic nature indicated by the linear polarization, the level structure of the ^{64}Cu nucleus was constructed and compared with the theoretical calculations. The results therefrom are presented and discussed in the next section.

III. RESULTS AND DISCUSSION

The level scheme of ^{64}Cu, as established from the current investigation, is illustrated in Fig. 5 while the list of levels and γ-ray transitions, along with their spectroscopic properties, is recorded in Table I. Figures 6 and 7 present typical gated spectra, from γ-γ matrix and γ-γ-γ cube respectively, showing the coincident γ rays constituting the level structure of ^{64}Cu. The level scheme has been extended up to an excitation energy $E_x \sim 6$ MeV and spin $\sim 10\hbar$. More than 50 new transitions were identified and placed in the scheme in addition to confirming or modifying the placements of the existing ones from previous studies [4]. In the case of the 1894-keV transition, de-exciting the 5084-keV state, the placement has been modified from that proposed in the previous work [4] while the transitions 1099 and 1532 keV that were reported by Chan *et al.* as "not placed" ones have been positioned in the excited scheme of the nucleus, following this analysis. Placements have also been revised for the 1374- and 1905-keV transitions with respect to the earlier observations in (n,γ) and $(p,n\gamma)$ studies [11]. The level structure is typical of shell-model configurations manifested in the complex, irregular excitation pattern therein. The spin-parity assignments to the states were made from the R_{ADO} and polarization asymmetry measurements of the depopulating γ-ray transitions. The latter was limited by lack of statistics owing to the modest number of detectors at 90° in the present experimental setup and could be carried out only for a limited number of transitions. Some of the levels, for which the polarization asymmetry of the de-exciting γ-ray transition could not be determined, were assigned parity

TABLE I. Details of the γ-ray transitions in ^{64}Cu observed in the present work. The level energies are accurate within 1 keV while the γ-ray energies within 0.5 keV for $E_\gamma < 1$ MeV, within 0.7 keV for 1 MeV $\leqslant E_\gamma \leqslant 2$ MeV, and within 1 keV for $E_\gamma > 2$ MeV. The R_{ADO} was determined in pure dipole gates. The relative intensities (I_γ) of the γ-ray transitions were determined with gate on 159- and 278-keV transitions.

E_i (keV)	E_γ (keV)	E_f (keV)	I_γ	J_i^π	J_f^π	R_{ADO}	$\Delta_{(pol)}$	P	γ-ray Assignment
158.8	158.8	0.0		2^+	1^+				$M1(+E2)$[a]
277.9	118.8	158.8		2^+	2^+				
	277.9	0.0			1^+	1.00 ± 0.47	-0.021 ± 0.025	-0.125 ± 0.155	$M1 + E2$
342.2	342.2	0.0		1^+	1^+				$D(+Q)$[a]
361.5	84.0	277.9	6.4 ± 0.8	3^+	2^+				
	202.7	158.8	1039.4 ± 5.0		2^+				$M1 + E2$[a]
	361.7	0.0			1^+				
573.6	212.1	361.5	1000.0 ± 0.0	4^+	3^+				$M1 + E2$[a]
	415.1	158.8	33.6 ± 5.5		2^+				
607.7	265.5	342.2		2^+	1^+				
	607.7	0.0			1^+				
662.5	384.6	277.9	19.5 ± 2.3	1^+	2^+	0.85 ± 0.13			$D(+Q)$
	662.5	0.0			1^+				
736.9	459.0	277.9	21.6 ± 3.7	2^+	2^+	0.76 ± 0.10			D
	578.4	158.8			2^+				
745.6	137.5	607.7		3^+	2^+				
	467.7	277.9	22.1 ± 3.0		2^+	0.89 ± 0.03	-0.005 ± 0.018	-0.040 ± 0.144	$M1 + E2$
	384.0	361.5	1.9 ± 0.4		3^+	0.87 ± 0.08			D
773.9	412.4	361.5	9.9 ± 6.0	(1)	3^+	1.52 ± 0.13			Q
820.0	458.5	361.5		(4)	3^+	0.86 ± 0.07			D
876.4	534.2	342.2		$(0)^+$	1^+	0.67 ± 0.10			$D + Q$[a]
	876.4	0.0			1^+				
895.2	320.6	573.6	18.9 ± 1.5	$(3)^+$	4^+	1.00 ± 0.11			$D + Q$[a]
	533.3	361.5	12.3 ± 1.3		3^+	0.97 ± 0.13			$D + Q$
	617.3	277.9	15.6 ± 0.9		2^+	0.68 ± 0.04			$M1 + E2$[a]
	895.2	0.0			1^+				
926.0	926.0	0.0		1^+	1^+				
1096.0	937.2	158.8	6.0 ± 4.4	2^+	2^+	0.89 ± 0.13			$D + Q$
1239.0	877.5	361.5		3^+	3^+				
	962.0	277.9			2^+				
1242.0	1242.0	0.0		$\leqslant 3$[a]	1^+				
1289.9	947.7	342.2		2^+	1^+	0.81 ± 0.24			D
1353.0	991.5	361.5	46.0 ± 1.2	4^+	3^+	1.12 ± 0.05	-0.029 ± 0.119	-0.521 ± 2.171	$M1 + E2$
	1075.7	277.9			2^+				
1434.9	861.3	573.6	8.4 ± 3.1	4^+	4^+	1.14 ± 0.11			$D + Q$
1460.5	565.3	895.2	13.1 ± 4.3	4^-	$(3)^+$				
	1098.9	361.5	15.9 ± 8.3		3^+	0.89 ± 0.08			$D + Q$
1592.5	1018.9	573.6	710.6 ± 4.2	6^-	4^+				$M2 + E3$[a]
	1231.2	361.5	7.4 ± 0.7		3^+				
	1314.7	277.9	22.4 ± 6.4		2^+	0.78 ± 0.04			
1615.0	1041.4	573.6	19.3 ± 0.9	5^-	4^+	0.93 ± 0.05			$D + Q$
1704.9	959.3	745.6	16.1 ± 0.6	4^+	3^+	0.77 ± 0.02	-0.017 ± 0.012	-0.291 ± 0.290	$M1 + E2$
1735.2	1161.6	573.6	42.7 ± 2.8	4^+	4^+	0.68 ± 0.02	-0.001 ± 0.024	-0.024 ± 0.568	$M1 + E2$
	1374.4	361.5	6.2 ± 1.7		3^+				
1769.3	1195.5	573.6	21.9 ± 0.9	5^+	4^+				
	1407.8	361.5	21.0 ± 0.9		3^+	1.13 ± 0.12			Q
1905.3	1331.7	573.6	36.2 ± 5.0	4^+	4^+	0.97 ± 0.04			$D + Q$
1924.0	1350.4	573.6	6.9 ± 1.4		4^+				
1978.3	1616.8	361.5	43.2 ± 1.3	5^+	3^+	1.22 ± 0.04			Q
2018.5	313.6	1704.9	9.7 ± 6.9	4^+	4^+	0.87 ± 0.04			D
2071.7	479.2	1592.5	137.9 ± 14.5	5^-	6^-	0.87 ± 0.03	-0.018 ± 0.026	-0.145 ± 0.219	$M1 + E2$

TABLE I. (*Continued.*)

E_i(keV)	E_γ(keV)	E_f(keV)	I_γ	J_i^π	J_f^π	R_{ADO}	$\Delta_{(pol)}$	P	γ-ray Assignment
2090.6	629.7	1460.5	22.2 ± 2.0	4^-	4^-	0.98 ± 0.06			$D+Q$
	1195.6	895.2	10.7 ± 1.4		$(3)^+$				
	1517.0	573.6	8.4 ± 0.7		4^+	0.76 ± 0.07			$D+Q$
2250.6	1677.0	573.6	25.0 ± 1.2	5^+	4^+	1.04 ± 0.03	−0.004 ± 0.043	−0.262 ± 2.887	$M1+E2$
2321.5	249.8	2071.7	27.4 ± 0.5	5^-	5^-	0.83 ± 0.03	−0.039 ± 0.042	−0.222 ± 0.251	$M1+E2$
2376.2	783.7	1592.5	182.4 ± 10.5	7^-	6^-	0.71 ± 0.01	−0.029 ± 0.007	−0.377 ± 0.235	$M1+E2$
2385.7	314.0	2071.7	82.8 ± 14.5	6^-	5^-	0.95 ± 0.10			$D+Q$
2414.2	1840.6	573.6	4.4 ± 0.5		4^+				
2434.9	1861.3	573.6	10.2 ± 0.6		4^+				
2497.1	478.6	2018.5	7.8 ± 15.2	5^+	4^+	0.67 ± 0.07			$D+Q$
2516.9	426.3	2090.6	8.6 ± 2.7	5^-	4^-	0.83 ± 0.12			$D+Q$
2582.3	2008.7	573.6	2.2 ± 0.7	5^-	4^+	0.98 ± 0.05			$D+Q$
2646.9	575.2	2071.7	14.5 ± 0.4	(5)	5^-	0.69 ± 0.06			$D+Q$
2689.6	313.4	2376.2	19.9 ± 1.0	6^-	7^-	0.85 ± 0.06			D
2715.1	1122.6	1592.5	80.9 ± 1.2	7^-	6^-	1.02 ± 0.07			$D+Q$
2810.0	1040.7	1769.3	17.0 ± 1.4	6^-	5^+	0.80 ± 0.08			D
2913.2	2339.6	573.6		5^-	4^+	0.82 ± 0.04			D
2924.3	538.6	2385.7	26.5 ± 5.2	6^-	6^-	0.87 ± 0.03	−0.035 ± 0.025	−0.310 ± 0.261	$M1+E2$
2948.1	562.4	2385.7	15.9 ± 2.8	5^-	6^-	0.91 ± 0.04			$D+Q$
2964.1	578.4	2385.7	3.6 ± 0.7	5^-	6^-	0.66 ± 0.05			$D+Q$
3049.7	664.0	2385.7	13.9 ± 2.5	7^-	6^-	0.93 ± 0.03	−0.050 ± 0.019	−0.539 ± 0.340	$M1+E2$
3124.2	200.1	2924.3		7^-	6^-				
	313.5	2810.0	11.2 ± 7.9		6^-	0.93 ± 0.06			$D+Q$
	434.6	2689.6	14.3 ± 3.9		6^-	0.99 ± 0.07	−0.022 ± 0.035	−0.166 ± 0.272	$M1+E2$
	738.5	2385.7	11.5 ± 1.0		6^-	0.93 ± 0.07			$D+Q$
3175.5	789.8	2385.7	10.0 ± 1.8		6^-				
3189.1	813.4	2376.2	43.3 ± 2.6	8^-	7^-	0.90 ± 0.03	−0.020 ± 0.025	−0.272 ± 0.376	$M1+E2$
	1596.6	1592.5	117.4 ± 1.6		6^-	1.10 ± 0.01	0.043 ± 0.011	2.266 ± 4.338	$E2+M3$
3267.0	881.3	2385.7	3.9 ± 0.7		6^-				
3276.8	561.7	2715.1			7^-				
3350.0	402.0	2948.1	8.6 ± 1.4	6^-	5^-	0.99 ± 0.10			$D+Q$
3375.2	878.1	2497.1		6^-	5^+	0.98 ± 0.06			$D+Q$
3486.6	771.5	2715.1	14.3 ± 1.6	8^-	7^-	0.92 ± 0.06			$D+Q$
3603.9	228.7	3375.2		7^-	6^-	0.96 ± 0.07			$D+Q$
	478.6	3124.2	29.2 ± 4.3		7^-				
	679.2	2924.3	14.0 ± 3.7		6^-	0.89 ± 0.04			$D+Q$
	1218.4	2385.7	12.2 ± 2.6		6^-	0.95 ± 0.04	−0.011 ± 0.026	−0.285 ± 0.732	$M1+E2$
	1282.4	2321.5	14.4 ± 2.1		5^-	1.13 ± 0.05	0.031 ± 0.033	0.896 ± 1.369	$E2+M3$
	1531.9	2071.7	13.2 ± 0.3		5^-	0.57 ± 0.03	0.017 ± 0.034	0.781 ± 2.036	$E2+M3$
3679.9	2087.4	1592.5	3.0 ± 0.4		6^-				
3685.0	2092.5	1592.5	4.0 ± 0.5	7^-	6^-	0.90 ± 0.08			$D+Q$
3732.1	1355.9	2376.2	7.5 ± 1.6		7^-				
3797.9	311.3	3486.6		9^-	8^-	0.80 ± 0.11			D
	608.8	3189.1	95.0 ± 1.5		8^-	0.98 ± 0.02	−0.024 ± 0.014	−0.237 ± 0.179	$M1+E2$
	1422.4	2376.2	11.5 ± 0.7		7^-	1.18 ± 0.09			Q
	2206.4	1592.5	6.5 ± 0.6		6^-				
3985.7	1609.5	2376.2	49.0 ± 1.3	9^-	7^-	1.25 ± 0.02	0.016 ± 0.017	0.867 ± 1.925	$E2$
4159.5	1469.9	2689.6	2.8 ± 0.6		6^-				
4162.7	1786.5	2376.2	2.6 ± 1.3		7^-				
4165.7	561.8	3603.9	6.2 ± 1.9	9^-	7^-				
	1789.5	2376.2	18.0 ± 1.9		7^-	1.26 ± 0.04			Q
4268.3	664.4	3603.9	6.1 ± 2.0		7^-				
4357.9	560.0	3797.9	19.3 ± 5.6		9^-				
4550.0	1360.9	3189.1	7.2 ± 1.6		8^-				
4555.0	2178.0	2376.2			7^-				
4566.8	580.5	3985.7		10^-	9^-				
	1377.7	3189.1	25.8 ± 2.3		8^-	1.16 ± 0.07	0.056 ± 0.025	1.061 ± 1.806	$E2$

TABLE I. (*Continued.*)

E_i(keV)	E_γ(keV)	E_f(keV)	I_γ	J_i^π	J_f^π	R_{ADO}	$\Delta_{(pol)}$	P	γ-ray Assignment
4689.7	2313.5	2376.2			7^-				
4896.3	1098.4	3797.9	30.1 ± 7.8	10^-	9^-	1.02 ± 0.04	-0.015 ± 0.015	-0.325 ± 0.428	$M1 + E2$
5083.5	1894.4	3189.1	22.0 ± 5.3	(9)	8^-	1.03 ± 0.08			$D + Q$
5093.7	1904.6	3189.1	6.0 ± 0.6	(9)	8^-	0.94 ± 0.22			$D + Q$
5684.3	1886.4	3797.9	3.2 ± 1.0	(11)	9^-	1.33 ± 0.10			Q
5910.4	2112.5	3797.9			9^-				
5915.3	2117.4	3797.9	3.8 ± 0.5	(10)	9^-	1.07 ± 0.13			$D + Q$
6068.0	2270.1	3797.9	3.8 ± 0.5	(10)	9^-	0.71 ± 0.03			$D + Q$

[a]Adopted from NNDC [11].
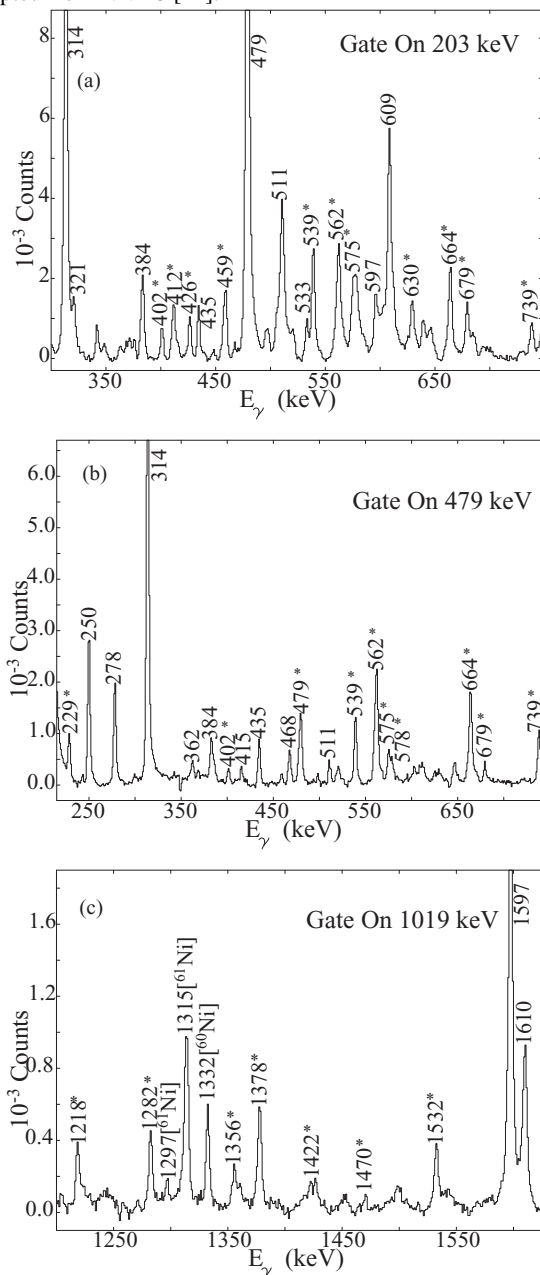
FIG. 6. Representative spectra with gate on γ-ray transitions of ^{64}Cu. The new transitions, first observed in the present study, are labeled with an asterisk (*).

FIG. 7. Sum spectrum of γ-γ gates, applied on the γ-γ-γ cube, from a list of transitions, 203, 212, 1019, 784, 813, 609, and 1597 keV, that illustrates the high-energy γ rays of ^{64}Cu.

based on a comparison with the results of the shell-model calculations after validation of the same. It is important to note that in view of the possible deorientation [12] of the ^{64}Cu nuclei at the 1593-keV ($J^\pi = 6^-$) $\tau \sim 30$ ns isomer [11], the R_{ADO} and P values of the transitions de-exciting the level were not calculated in the present study. The multipolarity and electromagnetic assignments of these γ rays have been adopted from the existing literature [4,11].

The single-particle configurations associated with the states of ^{64}Cu ($Z = 29, N = 35$), with 1 proton and 7 neutrons outside the ^{56}Ni ($Z = 28, N = 28$) core can be envisaged to be built on the occupancy of $f_{5/2}$, $p_{3/2}$, and $p_{1/2}$ orbitals at the lowest energies followed by excitations into the $g_{9/2}$ orbital in the higher energy domain. The occupation of fp orbitals by the single proton coupled to an odd number of neutrons, in the low-energy regime, is manifested in the positive-parity states observed in the level structure of the nucleus at these energies. It follows that the negative-parity states would involve occupation of $g_{9/2}$ orbital. In the previous studies [4] of the nucleus, the 1593-keV 6^- state was identified as the lowest negative-parity level in its excitation pattern. However, in the current investigation, the state at 1461 keV has been established as the lowest negative-parity state with $J^\pi = 4^-$, following the R_{ADO} measurement of the 1099-keV γ-ray transition de-exciting the level, as well as from comparison with the
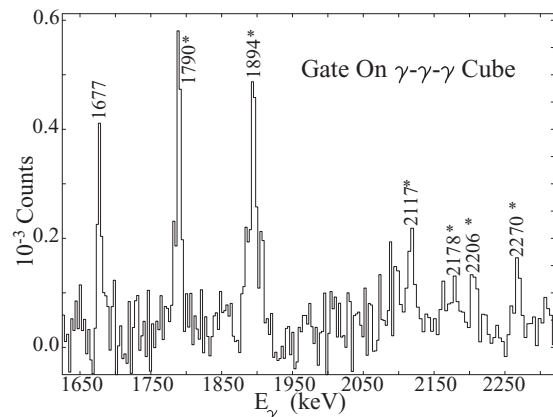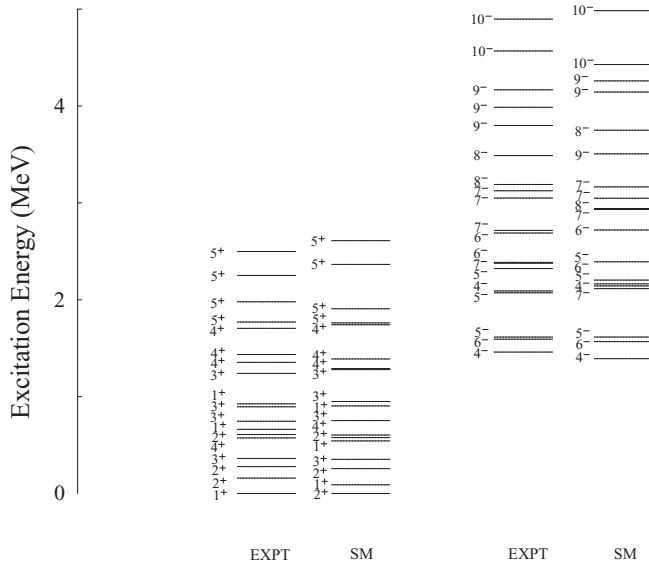
FIG. 8. Comparison between the experimental and calculated (SM) level energies of ^{64}Cu.

shell-model calculations (elaborated hereafter). The 565-keV γ-ray transition has also been confirmed to be de-exciting the same level from the present data. It may be noted that the level, along with the transitions therefrom, was identified in the previous studies with (n,γ) and $(p,n\gamma)$ reactions [11], albeit with tentative spin-parity assignment of 2^-. However, it is also not clear if the earlier investigations probed the coincidence relationships of the 1099- and 565-keV γ rays, that have now been established here. The same also holds for the 1408-keV transition listed in the (n,γ)- and $(p,n\gamma)$-induced studies [11].

In order to confirm the aforesaid propositions on the structure of the excited states of ^{64}Cu, large-basis shell-model calculations were carried out for the nucleus using the NUSHELLX (MSU) code [13]. The model space used therein consisted of orbitals $f_{5/2}$, $p_{3/2}$, $p_{1/2}$, and $g_{9/2}$ outside the ^{56}Ni core. The interaction deployed was $jj44bpn$ from Lisetskiy *et al.* [14]. The calculations were unrestricted with the eight valence nucleons (one proton and seven neutrons) allowed to occupy any orbital in the model space. Figure 8 presents a comparison between the calculated and the experimental level energies wherefrom it may be stated that the compliance between the two is satisfactory, albeit better for the positive-parity states vis-à-vis the negative-parity ones for which the agreement, particularly for the higher spin states, is within $\sim$250 keV for most of the levels. It is noted that the ordering of the ground state (1^+) and the first excited state (2^+) is swapped in the calculations. This points to the need for a slight reordering in the single-particle level spacings, which is beyond the scope of this work. The same has also been observed in some of the similar calculations in this region [15]. Table II summarizes the configurations of yrast positive- and negative-parity states in ^{64}Cu. The same indeed indicates the positive-parity states of the nucleus to be based on fp configurations while the negative-parity ones to be built on a neutron excitation into the $g_{9/2}$ orbital. The findings are commensurate with those in

TABLE II. Representative shell-model configurations in ^{64}Cu.

	J^π	$E_{\rm expt}$ (keV)	$E_{\rm SM}$ (keV)	Particles	Configurations			
	1^+	0.0	90.0	p	$f^0_{5/2}$	$p^1_{3/2}$	$p^0_{1/2}$	$g^0_{9/2}$
				n	$f^3_{5/2}$	$p^3_{3/2}$	$p^1_{1/2}$	$g^0_{9/2}$
	2^+	158.8	0.0	p	$f^0_{5/2}$	$p^1_{3/2}$	$p^0_{1/2}$	$g^0_{9/2}$
Positive				n	$f^3_{5/2}$	$p^3_{3/2}$	$p^1_{1/2}$	$g^0_{9/2}$
parity	3^+	361.5	353.0	p	$f^0_{5/2}$	$p^1_{3/2}$	$p^0_{1/2}$	$g^0_{9/2}$
				n	$f^3_{5/2}$	$p^3_{3/2}$	$p^1_{1/2}$	$g^0_{9/2}$
	4^+	573.6	604.0	p	$f^0_{5/2}$	$p^1_{3/2}$	$p^0_{1/2}$	$g^0_{9/2}$
				n	$f^3_{5/2}$	$p^3_{3/2}$	$p^1_{1/2}$	$g^0_{9/2}$
	5^+	1769.3	1761.0	p	$f^1_{5/2}$	$p^0_{3/2}$	$p^0_{1/2}$	$g^0_{9/2}$
				n	$f^3_{5/2}$	$p^3_{3/2}$	$p^1_{1/2}$	$g^0_{9/2}$
	4^-	1460.5	1392.0	p	$f^0_{5/2}$	$p^1_{3/2}$	$p^0_{1/2}$	$g^0_{9/2}$
				n	$f^3_{5/2}$	$p^3_{3/2}$	$p^0_{1/2}$	$g^1_{9/2}$
	5^-	1615.0	1615.0	p	$f^0_{5/2}$	$p^1_{3/2}$	$p^0_{1/2}$	$g^0_{9/2}$
				n	$f^3_{5/2}$	$p^3_{3/2}$	$p^0_{1/2}$	$g^1_{9/2}$
Negative	6^-	1592.5	1568.0	p	$f^0_{5/2}$	$p^1_{3/2}$	$p^0_{1/2}$	$g^0_{9/2}$
parity				n	$f^2_{5/2}$	$p^3_{3/2}$	$p^1_{1/2}$	$g^1_{9/2}$
	7^-	2376.2	2115.0	p	$f^1_{5/2}$	$p^0_{3/2}$	$p^0_{1/2}$	$g^0_{9/2}$
				n	$f^3_{5/2}$	$p^2_{3/2}$	$p^1_{1/2}$	$g^1_{9/2}$
	8^-	3189.1	2942.0	p	$f^0_{5/2}$	$p^1_{3/2}$	$p^0_{1/2}$	$g^0_{9/2}$
				n	$f^2_{5/2}$	$p^3_{3/2}$	$p^1_{1/2}$	$g^1_{9/2}$
	9^-	3797.9	3506.0	p	$f^1_{5/2}$	$p^0_{3/2}$	$p^0_{1/2}$	$g^0_{9/2}$
				n	$f^3_{5/2}$	$p^3_{3/2}$	$p^0_{1/2}$	$g^1_{9/2}$
	10^-	4566.8	4428.0	p	$f^0_{5/2}$	$p^1_{3/2}$	$p^0_{1/2}$	$g^0_{9/2}$
				n	$f^2_{5/2}$	$p^3_{3/2}$	$p^1_{1/2}$	$g^1_{9/2}$

the neighboring even-A Cu isotopes ^{62,66}Cu [2,16], the level structures of which have also been ascribed to the single-particle excitations in the fpg space.

It can be asserted that the level structure of ^{64}Cu nucleus, up to the excitation established from the present study, is entirely constituted of shell-model configurations. No evidence of collectivity or states based on broken ^{56}Ni core have been observed in this investigation. Beyond the observation of negative-parity states that could be ascribed to a neutron excitation (Table II) to $g_{9/2}$, it is envisaged that excitation of a second neutron to the same orbital would result in positive-parity states at higher excitation energies. The states in ^{64}Cu observed around $E_x \sim 6$ MeV, that are depopulated by high-energy γ-ray transitions, may actually represent such excitations. However, in the absence of the polarization measurement for these transitions, owing to statistical limitations, the exact nature of these levels could not be confirmed from the present efforts.

IV. CONCLUSION

Excited states of ^{64}Cu was studied following their population in heavy-ion-induced fusion-evaporation reaction and using an array of Compton-suppressed Clovers as the detection

system. Energy, intensity, coincidence relationships, angular correlation, and linear polarization of the emitted γ rays were determined for constructing the level scheme of the nucleus. More than 50 new γ-ray transitions were identified and the excitation scheme of the nucleus was established up to an energy $E_x \sim 6$ MeV and spin $\sim 10\hbar$. The experimentally observed states were compared with those from an unrestricted large-basis shell-model calculation and the overlap was found to be satisfactory. The compliance is indicative of the single-particle configurations underlying the excitation scheme of the nucleus to the extent studied in the present work.

[1] A. K. Singh, G. Gangopadhyay, D. Banerjee, R. Bhattacharya, R. K. Bhowmik, S. Muralithar, R. P. Singh, A. Mukherjee, U. D. Pramanik, A. Goswami *et al.*, Phys. Rev. C **59**, 2440 (1999).

[2] B. Mukherjee, S. Muralithar, R. P. Singh, R. Kumar, K. Rani, and R. K. Bhowmik, Phys. Rev. C **63**, 057302 (2001).

[3] D. A. Torres, F. Cristancho, L. L. Andersson, E. K. Johansson, D. Rudolph, C. Fahlander, J. Ekman, R. du Rietz, C. Andreoiu, M. P. Carpenter *et al.*, Phys. Rev. C **78**, 054318 (2008).

[4] T. U. Chan, M. Agard, J. F. Bruandet, A. Giorni, and J. P. Longequeue, Nucl. Phys. A **257**, 413 (1976).

[5] P. W. Green and D. M. Sheppard, Nucl. Phys. A **274**, 125 (1976).

[6] J. Bleck, R. Butt, K. H. Lindenberger, W. Ribbe, and W. Zeitz, Nucl. Phys. A **197**, 620 (1972).

[7] R. Palit, S. Saha, J. Sethi, T. Trivedi, S. Sharma, B. S. Naidu, S. Jadhav, R. Donthi, P. B. Chavan, H. Tan *et al.*, Nucl. Instrum. Methods Phys. Res., Sect. A **680**, 90 (2012).

[8] D. C. Radford, Nucl. Instrum. Methods Phys. Res., Sect. A **361**, 297 (1995).

[9] M. Piiparinen, A. Atac, J. Blomqvist, G. B. Hagemann, B. Herskind, R. Julin, S. Juutinen, A. Lampinen, J. Nyberg, G. Sletten *et al.*, Nucl. Phys. A **605**, 191 (1996).

[10] R. Palit, H. C. Jain, P. K. Joshi, S. Nagaraj, B. V. T. Rao, S. N. Chintalapudi, and S. S. Ghugre, Pramana **54**, 347 (2000).

[11] www.nndc.bnl.gov

[12] B. Crowell, P. Chowdhury, D. J. Blumenthal, S. J. Freeman, C. J. Lister, M. P. Carpenter, R. G. Henry, R. V. F. Janssens, T. L. Khoo, T. Lauritsen *et al.*, Phys. Rev. C **53**, 1173 (1996).

[13] B. A. Brown and B. Wildenthal, Annu. Rev. Nucl. Part. Sci. **38**, 29 (1988).

[14] A. F. Lisetskiy, B. A. Brown, M. Horoi, and H. Grawe, Phys. Rev. C **70**, 044314 (2004).

[15] F. Kearns, L. P. Ekstrom, G. D. Jones, T. P. Morrison, O. M. Mustaffa, H. G. Price, D. N. Simister, P. J. Twin, R. Wadsworth, and N. J. Ward, J. Phys. G **6**, 1131 (1980).

[16] P. Singh, R. Palit, D. Choudhury, P. C. Srivastava, S. Biswas, S. Saha, and J. Sethi, Eur. Phys. J. A **53**, 69 (2017).